Article

The Effect of Incubation near an Inversely Oriented Square Pyramidal Structure on Adsorption Properties of Horseradish Peroxidase

Yuri D. Ivanov [1,2,*], Vadim Yu. Tatur [3], Tatyana O. Pleshakova [1], Ivan D. Shumov [1], Andrey F. Kozlov [1], Anastasia A. Valueva [1], Irina A. Ivanova [1], Maria O. Ershova [1], Nina D. Ivanova [3,4], Igor N. Stepanov [3], Andrei A. Lukyanitsa [3] and Vadim S. Ziborov [1,2]

[1] Institute of Biomedical Chemistry, Pogodinskaya Str., 10 Build. 8, Moscow 119121, Russia; t.pleshakova1@gmail.com (T.O.P.); shum230988@mail.ru (I.D.S.); afkozlow@mail.ru (A.F.K.); varuevavarueva@gmail.com (A.A.V.); i.a.ivanova@bk.ru (I.A.I.); motya00121997@mail.ru (M.O.E.); ziborov.vs@yandex.ru (V.S.Z.)

[2] Joint Institute for High Temperatures of the Russian Academy of Sciences, Moscow 125412, Russia

[3] Foundation of Perspective Technologies and Novations, Moscow 115682, Russia; v_tatur@mail.ru (V.Y.T.); ninaivan1972@gmail.com (N.D.I.); stepanovigorn@gmail.com (I.N.S.); andrei_luk@mail.ru (A.A.L.)

[4] Moscow State Academy of Veterinary Medicine and Biotechnology Named after Skryabin, Moscow 109472, Russia

* Correspondence: yurii.ivanov.nata@gmail.com

Featured Application: It is important to take into account the effect of the incubation of aqueous enzyme solutions near pyramidal structures on their adsorption properties revealed herein in the development of highly sensitive biosensor systems, especially enzyme-based ones.

Abstract: The incubation of a solution of horseradish peroxidase (HRP) enzyme either below the apex or near the base of an inversely oriented square pyramid (inverted square pyramid; ISP) has been found to influence the enzyme's aggregation and adsorption properties. The HRP enzyme is used herein as a model object due to its importance in analytical chemistry applications. Atomic force microscopy (AFM) is employed to investigate the HRP's adsorption on mica substrates at the single-molecule level. Conventional spectrophotometry is used in parallel as a reference method for the determination of the HRP's enzymatic activity. Using AFM, we reveal a significant change in the adsorption properties of HRP on mica substrates after the incubation of the HRP solutions either above the base or below the apex of the ISP in comparison with the control HRP solution. The same situation is observed after the incubation of the enzyme solution above the center of the ISP's base. Here, the enzymatic activity of HRP remained unaffected in both cases. Since pyramidal structures of positive and inverted orientation are employed in biosensor devices, it is important to take into account the results obtained herein in the development of highly sensitive biosensor systems, in which pyramidal structures are employed as sensor (such as AFM probes) or construction elements.

Keywords: atomic force microscopy; peroxidase; protein aggregation; electromagnetic field; inverted pyramid; enzyme-based biosensor; molecular absorption spectroscopy

1. Introduction

Single-molecule enzymology, which focuses on studying single enzyme molecules instead of their large ensembles, is increasing in popularity [1,2]. This approach utilizes so-called molecular detectors, which allow researchers to investigate enzymes with ultra-high sensitivity [3]: atomic force microscopes [4–7], nanoelectronic detectors [8–11], nanopore-based sensors [12,13], total internal reflection microscopes [2] etc.

It should be emphasized that enzymes are now widely employed in analytical chemistry [14–16]. For example, horseradish peroxidase (HRP) has been employed for the

detection of various heavy metal ions using microplate-based colorimetric analysis [14] and conventional spectrophotometry [15]. This enzyme has also been employed for the amperometric detection of phenolic compounds [16]. The importance of the HRP enzyme in analytical chemistry applications determined its use in our present research as a model object.

Pyramidal structures are employed in various biosensor devices [17–20]. Balezin et al. [21] performed a theoretical study demonstrating a change in the spatial distribution of an electromagnetic field near pyramidal structures. Moreover, these authors demonstrated that a change in the mutual orientation of a pyramid and in the direction of an incident electromagnetic field lead to a change in the topography of the spatial distribution of electromagnetic fields near the pyramid [21]. In our recent experimental study, a change in the aggregation state of an HRP enzyme upon its adsorption on mica after the incubation of its solution near such a structure was demonstrated using atomic force microscopy (AFM) [22]. One of the advantages of AFM consists in its visualization of the objects under study at the level of individual macromolecules [23]. Furthermore, this is the feature that makes AFM a very useful tool in single-molecule enzymology [3,4]. Due to its extremely high, single-molecule sensitivity, AFM is capable of revealing even subtle effects of external factors on the structure of biological objects [24], including enzyme macromolecules [25]. As such, by using AFM, it was demonstrated that electromagnetic fields of even a very low power density (of the order of 10^{-12} W/cm^2) can affect physicochemical properties of enzymes [26].

Regarding the interaction of electromagnetic fields with pyramidal structures, on the one hand, the incubation of HRP solution near a pyramidal structure has been shown to lead to the disaggregation of the enzyme [22]. Such an effect was ascribed to the concentration of an external electromagnetic field in certain points of space at the expense of a resonant interaction of the pyramidal structure with the field [21]. On the other hand, not only normal but also inverted pyramidal structures have been reported to be employed in biosensor devices [17,20]. Moreover, it should be noted that the effective scattering surface of a pyramidal structure can depend on the angle of incidence of the electromagnetic waves, and, accordingly, the spatial distribution of the electromagnetic fields near this structure can depend on its spatial orientation. In this regard, it is of interest to determine whether the incubation of an enzyme solution in the vicinity of an inverted pyramidal structure has an influence on its properties.

Herein, the influence of the incubation of an HRP enzyme solution near an inverted pyramidal structure (ISP) on the enzyme's adsorption properties was studied using AFM, while spectrophotometry was employed as a reference method. We performed these experiments in order to study whether the incubation of the enzyme solution near a pyramidal structure with different spatial orientation influences the enzyme's properties. The incubation of the HRP solution near the ISP's apex and above its base was found to induce an increased aggregation of the enzyme upon its adsorption on mica. The increased aggregation of HRP manifested itself in the form of an increase in both the height and lateral sizes of the AFM-visualized objects adsorbed on mica in comparison with those observed in control experiments. Here, the enzymatic activity of HRP remained unchanged in all experiments.

Since pyramidal structures of both normal and inverted orientation find their application in the construction of various biosensors, the results reported herein should be taken into account in the development of novel biosensor devices, including AFM-based systems employing pyramid-shaped tips. Our results can also be of use in the development of noise-protection systems for biosensors, including anechoic chambers with pyramidal elements.

2. Materials and Methods

2.1. Chemicals and Protein

HRP protein was purchased from Sigma (Cat. #6782). 2,2′-azino-bis(3-ethylbenzothia-zoline-6-sulfonate) (ABTS) was purchased from Sigma (Cat. #A1888). Salt mixture for the

preparation of Dulbecco's modified phosphate-buffered saline (PBSD) was purchased from Pierce (USA). Disodium hydrogen orthophosphate (Na_2HPO_4), citric acid and hydrogen peroxide (H_2O_2) were all of analytical or higher purity grade, and they were purchased from Reakhim (Moscow, Russia). In all our experiments, ultrapure deionized water (of 18.2 M$\Omega{\times}$cm resistivity), obtained using a Simplicity UV system (Millipore, Molsheim, France) was used.

2.2. Experimental Setup

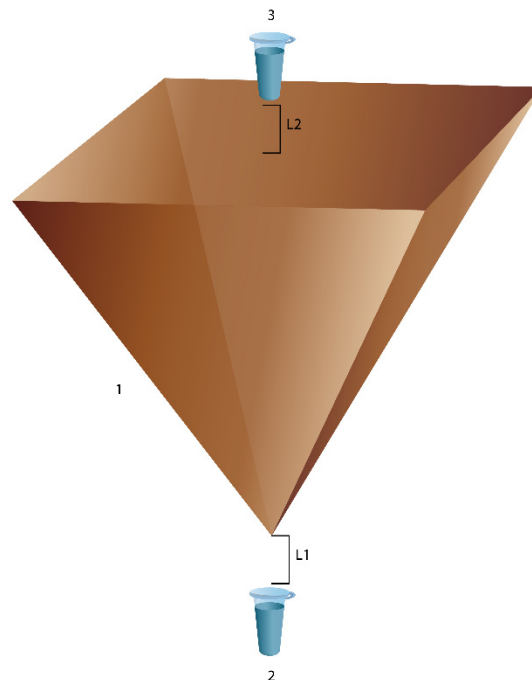Figure 1 displays a representation of the setup used in our experiments.

Figure 1. Experimental setup. Numbers indicate the main units of the setup: the ISP (1) and the test tube with the enzyme solution. The tube was placed either below the ISP's apex (2) or above its base (3). L_1 and L_2 represent the distance between the tube and the ISP's apex or the center of its base, respectively.

The ISP was made from dielectric (textolite) sheets coated with 2 mm layers of copper in order to provide efficient reflection of electromagnetic radiation. The height and the apex angle of the ISP were 130 mm and 52°, respectively. The size of the pyramid was selected so that the resonance occurs in the microwave range [21]. The Eppendorf-type tubes containing 1 mL of 0.1 µM solution of HRP in 2 mM PBSD buffer were placed either 1 cm below the ISP's apex or 1 cm above the ISP's base (positions 2 and 3 in Figure 1, respectively) and incubated there for 40 min. The distance between the pyramid and the samples, and the incubation time were the same as those in our previous study [22], so only the spatial orientation of the pyramid was changed. At the same time, control solutions of the enzyme were incubated at a much longer (three meters) distance from the ISP. The room in which the experiments were performed was not shielded from external electromagnetic radiation. At the same time, we did not use any additional equipment to intentionally generate electromagnetic radiation. After the incubation, mica substrates were immersed into the solutions of the enzyme in order to study its adsorption on mica using AFM. Each experiment was performed in at least three technical replicates. In parallel, the enzymatic activity of HRP against its substrate ABTS was estimated spectrophotometrically. These procedures are described below.

2.3. HRP Adsorption on Mica Substrates for AFM

In our experiments, adsorption of the HRP enzyme was performed directly from its solutions on mica substrates following the technique developed by Kiselyova et al. [27] analogously to [22,25,26]. The implementation of this technique is schematically shown in Figure 2.
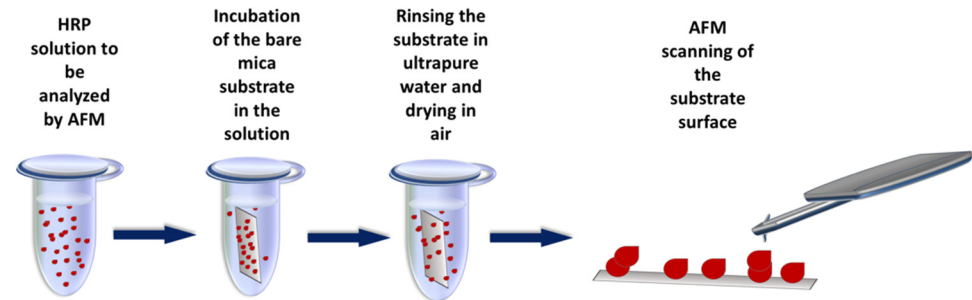

Figure 2. Schematic illustration of the direct surface adsorption of HRP from its aqueous solutions on mica substrates to study its adsorption using AFM.

In brief, both working solutions (incubated near the ISP) and control solutions (incubated three meters away from the ISP) were treated in one and the same way as follows: A freshly cleaved mica substrate (7 × 15 mm) was immersed into the test tube containing 1 mL of 0.1 μM HRP solution and incubated therein for ten minutes in a shaker at 600 rpm and at room temperature. Then, the substrates were rinsed with ultrapure water and dried in air.

We performed our experiments with 0.1 μM HRP solutions since, at higher concentrations, the adsorbed enzyme forms layer structures on the substrate surface, making the visualization of single enzyme molecules impossible.

Preliminary experiments were performed with the use of protein-free ultrapure water instead of protein solution; in these experiments, no objects with height greater than 0.5 nm were observed.

2.4. Atomic Force Microscopy Measurements

AFM measurements were performed in air analogously to our previous papers [22,25,26]. The AFM images were obtained with a Titanium multimode atomic force microscope (which pertains to the equipment of the "Human Proteome" Core Facility of the Institute of Biomedical Chemistry, supported by the Ministry of Education and Science of the Russian Federation, agreement 14.621.21.0017, unique project IDRFMEFI62117X0017; NT-MDT, Zelenograd, Russia) equipped with NSG10 cantilevers ("TipsNano", Zelenograd, Russia; 47–150 kHz resonant frequency, 0.35–6.1 N/m force constant). The microscope was operated in intermittent contact mode. The microscope was preliminarily calibrated using a TGZ1 calibration grating (NT-MDT, Russia; step height 21.4 ± 1.5 nm). The atomic force microscope was operated with the standard NOVA Px software (NT-MDT, Moscow, Zelenograd, Russia) supplied with the microscope.

For each substrate incubated in the HRP solution, the number of frames was ≥10, and the number of objects imaged in each sample was ≥500. The AFM images were obtained, treated and exported in ASCII format with the standard NOVA Px software (NT-MDT, Moscow, Zelenograd, Russia).

The relative density of the distribution of the imaged objects with height $\rho(h)$ was calculated as reported by Pleshakova et al. [28] as follows:

$$\rho(h) = (N_h/N) \times 100\% \tag{1}$$

In Equation (1), N_h is the number of AFM-imaged objects with height h, while N is the total number of AFM-imaged objects [28]. The so-calculated distributions are presented in the form of $\rho(h)$ curves (density function plots [28]).

The aggregation state of the HRP enzyme was characterized using parameter α, which was calculated as the ratio between the relative content of aggregates and that of monomers:

$$\alpha = \rho_2(h)/\rho_1(h) \tag{2}$$

where ρ_1 and ρ_2 are the values of the density of distributions, corresponding to monomeric and oligomeric (aggregated) HRP, respectively. For mica-adsorbed HRP, the density function plot $\rho(h)$ typically has two characteristic peaks corresponding to aggregated and monomeric HRP, respectively [25]. Accordingly, the α value was used to characterize the ratio between the content of aggregates and monomers.

In order to determine the relative content of HRP monomers and aggregates after adsorption on mica substrates, we performed an approximation of the experimental $\rho(h)$ curves using the root mean square method [7]:

$$\rho(h) = \rho_1(h) + \rho_2(h) = K_1 \frac{(h - m_1)^2}{b_1^2} \exp\left(\frac{-(h - m_1)^2}{2b_1^2} \right) + K_2 \frac{(h - m_2)^2}{b_2^2} \exp\left(\frac{-(h - m_2)^2}{2b_2^2} \right) \tag{3}$$

where K_1, m_1 and b_1 are the parameters of the distribution corresponding to monomers, and K_2, m_2 and b_2 are those corresponding to aggregates.

The number of AFM-visualized objects, normalized per 400 μm^2 area of the substrate surface (N_{norm}), was calculated according to [28] as follows:

$$N_{norm} = (N \times 400)/(n \times a^2) \tag{4}$$

where N is the number of objects visualized in one and the same experiment, n is the number of frames obtained in this experiment, and a is the linear frame size (μm).

In order to check whether the noise resulting from the unspecific adsorption from buffer solution is within its normal range (which typically makes up 500 objects per 400 μm^2 [29]), blank experiments with the use of pure buffer instead of HRP enzyme solution were performed. No objects with height >0.5 nm was observed on the mica surface in the blank experiments.

Objects visualized on the substrate surface using AFM were calculated using specialized AFM data processing software developed in the Institute of Biomedical Chemistry in collaboration with the Foundation of Perspective Technologies and Novations. Based on these calculations, the relative density of the distribution of the imaged objects with height $\rho(h)$ and histogram showing the height distributions of the number of AFM-visualized objects normalized per 400 μm^2 area of the substrate surface ($N_{norm}(h)$) were plotted.

2.5. Spectrophotometric Estimation of Enzymatic Activity

The functional activity of the HRP enzyme was estimated using a standard assay with ABTS as reported by Sanders et al. [30]. ABTS is commonly employed as an HRP substrate for the determination of the functional activity of this enzyme [31]. The assay was performed at pH 5.0 as recommended by the ABTS substrate manufacturer (Sigma) [31]. A 30 μL volume of 0.1 μM HRP solution was pipetted into a 3 mL quartz cell with a pathlength of 1 cm (Agilent, Germany), containing 2.96 mL of 0.3 mM ABTS solution in phosphate–citrate buffer (51 mM Na_2HPO_4, 24 mM citric acid, pH 5.0), and stirred thoroughly. Accordingly, the final HRP concentration in the cell was 1 nM. After that, a 8.5 μL volume of 3% (w/w) hydrogen peroxide was pipetted into the cell, and spectrum acquisition was started immediately. The enzymatic activity of HRP was calculated according to the manufacturer's recommendations [31].

3. Results

3.1. Analysis of AFM Data

Figure 3 displays typical AFM images (left) and corresponding cross-section profiles (right) of HRP adsorbed on mica from its solutions incubated either 1 cm below the ISP's apex (Figure 3a), 1 cm above the ISP's base (Figure 3b) or three meters away from the ISP (Figure 3c; control sample).
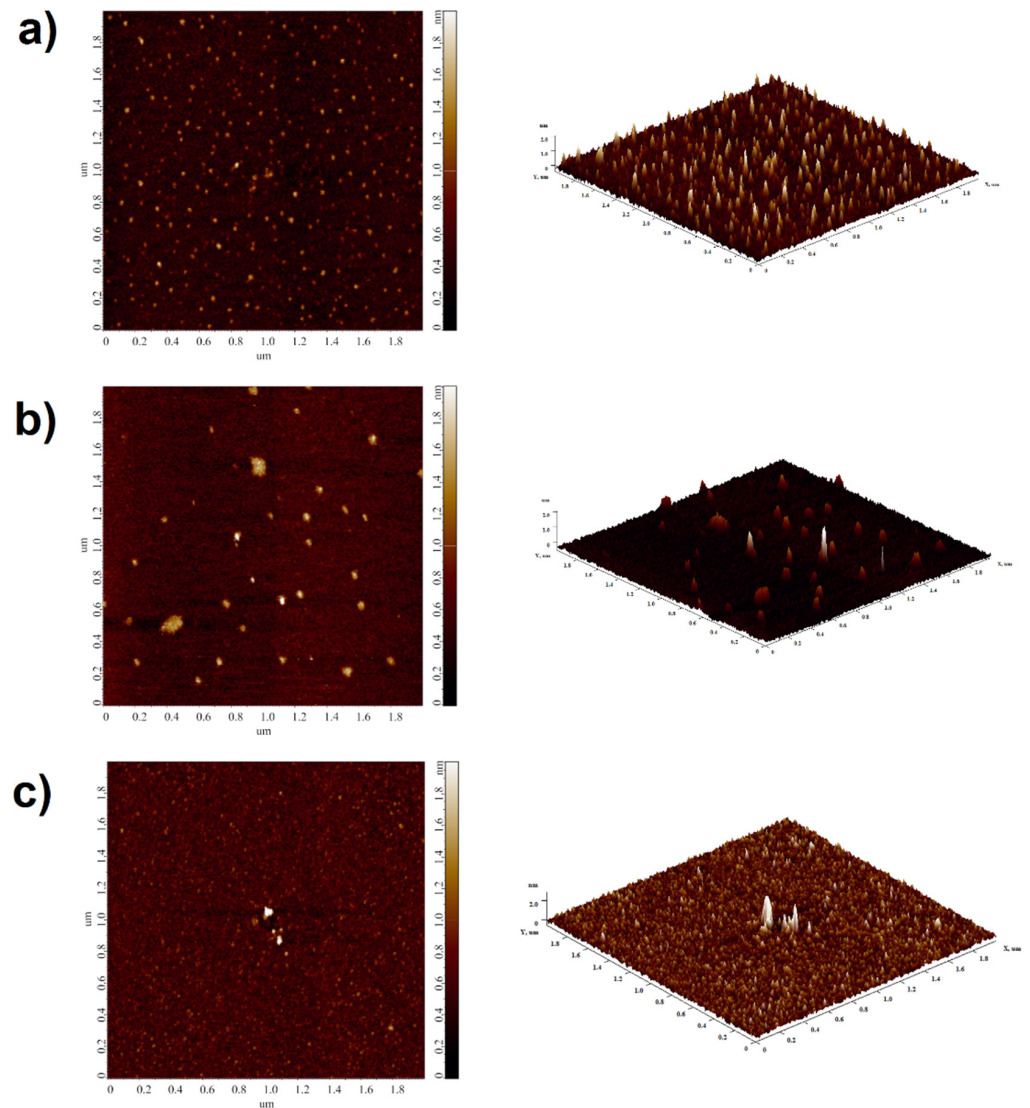

Figure 3. Typical AFM 2D (left) and 3D (right) images of HRP adsorbed on mica from its solutions incubated either 1 cm below the ISP's apex (**a**), 1 cm above the ISP's base (**b**) or three meters away from the ISP (**c**) (control sample). The scan size of all the images is 2 μm × 2 μm, Z scale is from 0 to 2 nm.

In all the AFM images shown in Figure 3, compact objects with heights >0.5 nm are visualized on the substrate surface. These objects can be attributed to adsorbed HRP. At the same time, no such objects were visualized on the mica surface in blank experiments with protein-free buffer.

Figure 4 displays $\rho(h)$ curves (Figure 4a) and $N_{norm}(h)$ histograms (Figure 4b) obtained after analysis of AFM data obtained in our experiments for HRP adsorbed on mica from the solutions incubated 1 cm below the ISP's apex (red), 1 cm above the ISP's base (green) or three meters away from the ISP (black; control sample).
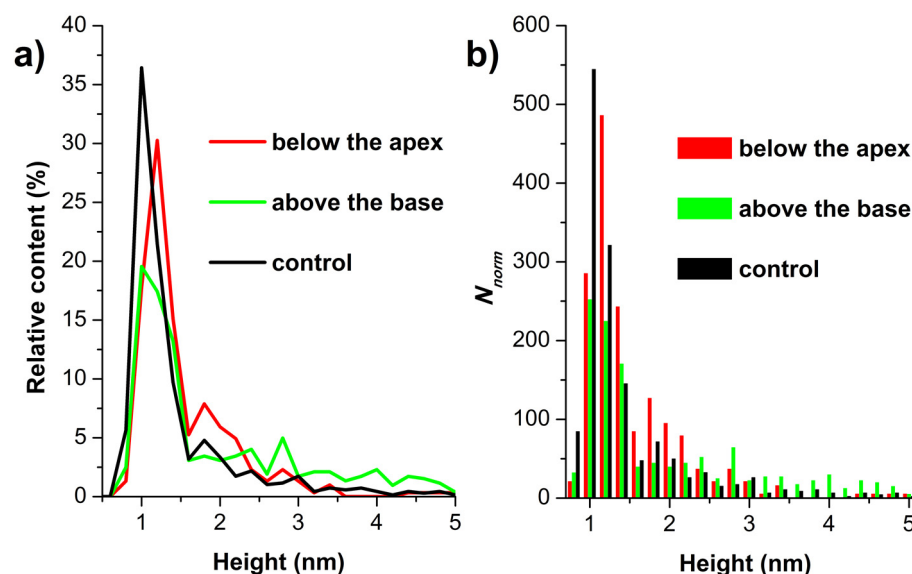
Figure 4. Results of processing the AFM data. $\rho(h)$ curves (**a**) and $N_{norm}(h)$ histograms (**b**) obtained after analysis of AFM data obtained in our experiments for HRP adsorbed on mica from the solutions incubated 1 cm below the ISP's apex (red), 1 cm above the ISP's base (green) or three meters away from the ISP (black; control sample).

The $\rho(h)$ curve obtained in the control experiments (Figure 4a, black curve) has two characteristic maxima at 1.0 ± 0.2 nm (h_{max1}) and 1.8 ± 0.2 nm (h_{max2}). In our previous papers, we justified that the objects of ~1.0 nm height correspond to a mica-adsorbed monomeric form of HRP, while the objects of 1.8 nm and greater heights correspond to its aggregated form [25,26]. In the control experiments, the α ratio amounted to $\rho_2/\rho_1 = 0.37$.

In contrast to the control HRP solutions, a significant increase in the α ratio was observed for the solutions incubated 1 cm below the ISP's apex (Figure 4a, red curve): $\rho_2/\rho_1 = 0.6$. This clearly indicates an increased aggregation of the enzyme adsorbed on mica from these solutions.

For the HRP solution incubated 1 cm above the ISP's base, several maxima are observed (Figure 4a, green curve). That is, while h_{max1} is still observed at 1.0 ± 0.2 nm, h_{max2} shifts to lower heights (1.4 ± 0.2 nm). Apart from these two peaks, a substantially broadened (1.8–3 nm) peak with the maximum shifted to 2.4 ± 0.4 nm (h_{max3}) is observed (Figure 4a, green curve). The $\rho(h)$ curve obtained for this solution indicates a decrease in the content of 1.0 nm-high monomeric HRP down to $\rho(h_{max1}) = 20\%$. This is in contrast to the case with the control solution, for which $\rho(h_{max1}) = 37\%$ was obtained.

The approximation of the experimental $\rho(h)$ curves allowed us to determine the integral relative content of the HRP aggregates after adsorption on mica substrates in our experiments. Table 1 summarizes the results of this approximation.

Table 1. Maximum heights of the $\rho(h)$ curves and relative content of HRP aggregates after adsorption on mica.

HRP Samples	h_{max1}, nm	h_{max2}, nm	% of Oligomers
Below the ISP's apex	1.2 ± 0.2	1.8 ± 0.2	38 ± 4
Above the ISP's base	1.0 ± 0.2	1.4 ± 0.2; 2.4 ± 0.4	45 ± 10
Control sample	1.0 ± 0.2	1.8 ± 0.2	27 ± 4

It should be noted that the number of mica-adsorbed objects N_{norm} normalized per 400 μm^2 is approximately similar in all (working and control) experiments with HRP solutions (Figure 4b).

3.2. Enzymatic Activity of HRP

The functional activity of the HRP enzyme was estimated using spectrophotometry in both working experiments (in which the enzyme solution was incubated either at a 1 cm distance below the pyramid's apex or in the center of its base) and control experiments (in which the solution was kept 10 m away from the pyramid), as described in the Materials and Methods Section. Figure 5 displays the time dependencies of the change in absorbance of 0.3 mM ABTS solution containing 1 nM HRP and 2.5 mM hydrogen peroxide ($A_{405}(t)$ curves).
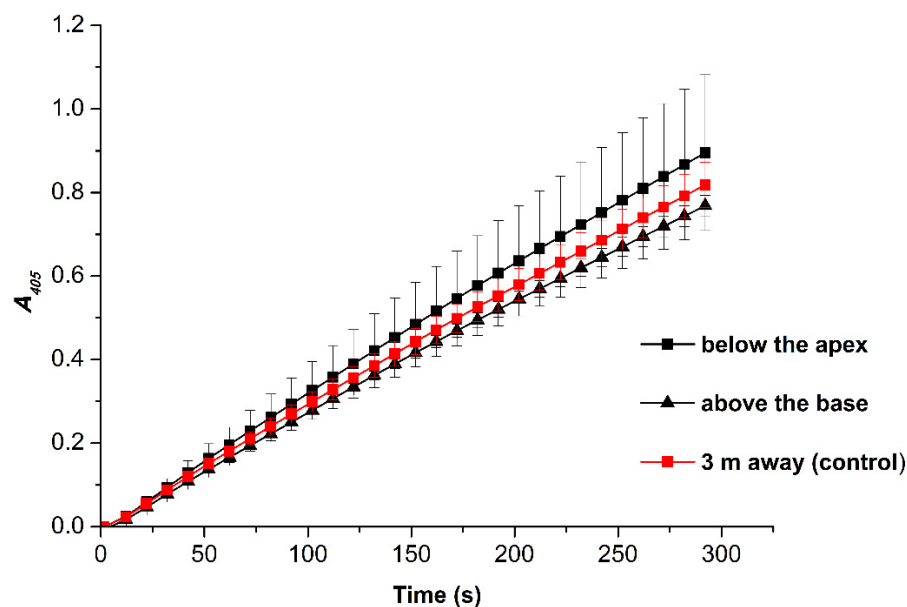

Figure 5. The time dependencies of the change in absorbance of 0.3 mM ABTS solution containing 1 nM HRP and 2.5 mM hydrogen peroxide. Experimental conditions: cell pathlength 1 cm, room temperature 25 °C.

According to the $A_{405}(t)$ curves obtained, virtually no difference in the enzyme's functional activity was observed in our experiments. This indicates that the incubation of the HRP solution near the pyramid does not affect the enzyme's activity against ABTS. In our experiments, the enzymatic activity of HRP was ~46 U/(mL enzyme).

4. Discussion

The influence of the incubation of an enzyme solution near an inverted pyramidal (ISP) structure on the enzyme adsorption properties was studied using AFM with the example of horseradish peroxidase. First, adsorption of HRP on mica from control solutions, incubated three meters away from the ISP, was studied. The number of mica-adsorbed objects, normalized per 400 μm² of the substrate surface, was calculated, and density functions $\rho(h)$ were plotted. Based on the ratio α between the relative content of monomeric HRP and that of oligomeric HRP on the mica surface, the aggregation state of the enzyme in the control solutions was estimated. Second, in the same way, these data were obtained for the HRP solutions incubated either 1 cm below the ISP's apex or 1 cm above the center of the ISP's base, and they were compared with the data for the control solutions.

For the HRP enzyme solution incubated for 40 min below the ISP's apex, an increased aggregation of HRP macromolecules upon the enzyme's adsorption on mica was observed in comparison with the control solution. Indeed, the relative content of oligomeric HRP increased up to 38 ± 4% (from 27 ± 4% in the case of the control solution; Table 1). Furthermore, the α value, which characterizes the ratio between the relative content of aggregates and that of monomers, increased from 0.37 to 0.6, clearly indicating an increased enzyme aggregation. Moreover, an increase in the contribution of objects with a height of

1.8 nm or more to the right wing of the relative distribution of adsorbed HRP with height was observed. These high objects are attributed to aggregated forms of HRP [22,25,26].

For the HRP solution incubated 1 cm above the ISP's base, an increased enzyme aggregation was observed: the relative content of aggregates increased up to $45 \pm 10\%$ (Table 1).

At the same time, no change in the normalized number of the mica-adsorbed objects was observed for the HRP solutions incubated below the apex or above the base of the ISP (Figure 4b).

Such changes in the adsorption properties of the HRP enzyme after the incubation near the ISP can be explained by an alteration in the spatial structure of the enzyme globule. This, accordingly, leads to a change in the interaction of HRP macromolecules both with the mica substrate surface, with each other (both in the solution and on the surface) and with the water solvent. Furthermore, alterations in the structure of the HRP globule do not affect its enzymatic activity against ABTS, which remained unchanged after the incubation of its solutions near the ISP. In this regard, it must be emphasized that spectrophotometry represents a macroscopic method, in which a signal, produced by a large number of enzyme macromolecules, is recorded. At the same time, AFM operates at the level of single macromolecules. Under the action of the AFM tip, a nanomechanically assisted excitation of an enzyme can be observed [32].

The effects on enzyme aggregation, observed in our present study, are most likely caused by a rather complex process connected with the influence of external re-distributed electromagnetic radiation on the enzyme. The latter, in turn, is surrounded by ice-like water structures in the solution. These structures can change under the action of the electromagnetic radiation of various wavelengths due to a change in the ratio between para- and ortho-isomers of water in the water/enzyme system [33]. That is, the observed effect is likely caused indirectly, being connected to a change in the ratio between para- and ortho-isomers of water in the hydration shell around the enzyme globule. Accordingly, other water-dissolved enzymes can also be affected by electromagnetic radiation upon their incubation near a pyramidal structure.

The effects observed herein differ from those of a normally oriented pyramidal structure, which were reported previously [22]. Such a difference in the effects on the protein solution from oppositely oriented pyramids can be due to the following circumstances: Firstly, a change in the mutual orientation of a pyramid and in the direction of an incident electromagnetic field lead to a different topography of the spatial distribution of the electromagnetic field near the pyramid [21]. According to the theoretical study by Minin et al. [34], the influence of pyramidal structures consists of the induction of changes in the topography of external electromagnetic fields near the pyramid at wavelengths comparable to the size of its face. This takes place at the expense of both refraction and reflection from the face of the pyramid. Moreover, a strong dependence of the effective scattering surface on the angle of incidence on the plane (which can be a model of the base of the pyramid) was shown [35]. It was emphasized that this effect can be also observed for more complex geometric solids [35]. Thus, the difference in the effects of pyramidal structures upon their different orientation in space on biological objects was grounded theoretically and confirmed in our experiments with the example of HRP.

The results obtained herein can be of use in the development of systems for the concentration of electromagnetic waves and in AFM studies employing pyramid-shaped tips [36]. Thus, AFM probes of pyramidal shape can have an impact on physicochemical properties of proteins or other biological objects studied in such biosensors, and this is what should be studied in the future. Our results can also be of interest for researchers developing various biosensors in which pyramidal structures are employed as either construction or sensitive elements.

5. Conclusions

The effect of an inverted pyramidal structure, simulating AFM pyramid-shaped tips, on physicochemical properties of an enzyme was demonstrated with the use of HRP as a model object. An increase in HRP aggregation upon adsorption of its macromolecules on mica AFM substrates from buffered solutions of this enzyme was observed. Our experiments indicate that the orientation of the pyramidal structure influences the effect on the HRP enzyme resulting from the incubation of its solution near this structure. The results obtained can be of use in the development of biosensor devices intended for the study of enzymes, proteins and other biological objects.

References

1. Perkel, J. Single molecule enzymology finds its stride. *BioTechniques* **2015**, *59*, 183–187. [CrossRef] [PubMed]
2. Gilboa, T.; Ogata, A.F.; Walt, D.R. Single-Molecule Enzymology for Diagnostics: Profiling Alkaline Phosphatase Activity in Clinical Samples. *ChemBioChem* **2022**, *23*, e202100358. [CrossRef] [PubMed]
3. Eghiaian, F.; Schaap, I.A.T. Structural and Dynamic Characterization of Biochemical Processes by Atomic Force Microscopy. In *Single Molecule Enzymology. Methods in Molecular Biology (Methods and Protocols)*; Mashanov, G., Batters, C., Eds.; Humana Press: Totowa, NJ, USA, 2011; Volume 778, pp. 71–95.
4. Xie, X.S.; Lu, H.P. Single-molecule enzymology. *J. Biol. Chem.* **1999**, *274*, 15967–15970. [CrossRef] [PubMed]
5. Ivanov, Y.D.; Bukharina, N.S.; Frantsuzov, P.A.; Pleshakova, T.O.; Kanashenko, S.L.; Medvedeva, N.V.; Argentova, V.V.; Zgoda, V.G.; Munro, A.W.; Archakov, A.I. AFM study of cytochrome CYP102A1 oligomeric state. *Soft Matter* **2012**, *8*, 4602–4608. [CrossRef]
6. Ivanov, Y.D.; Bukharina, N.S.; Pleshakova, T.O.; Frantsuzov, P.; Krokhin, N.V.; Ziborov, V.S.; Archakov, A.I. Atomic force microscopy visualization and measurement of the activity and physicochemical properties of single monomeric and oligomeric enzymes. *Biophysics* **2011**, *56*, 892–896. [CrossRef]
7. Ivanov, Y.D.; Frantsuzov, P.A.; Zöllner, A.; Medvedeva, N.V.; Archakov, A.I.; Reinle, W.; Bernhardt, R. Atomic Force Microscopy Study of Protein–Protein Interactions in the Cytochrome CYP11A1 (P450scc)-Containing Steroid Hydroxylase System. *Nanoscale Res. Lett.* **2010**, *6*, 54. [CrossRef] [PubMed]
8. Malsagova, K.A.; Pleshakova, T.O.; Galiullin, R.A.; Kaysheva, A.L.; Shumov, I.D.; Ilnitskii, M.A.; Popov, V.P.; Glukhov, A.V.; Archakov, A.I.; Ivanov, Y.D. Ultrasensitive nanowire-based detection of HCVcoreAg in the serum using a microwave generator. *Anal. Methods* **2018**, *10*, 2740–2749. [CrossRef]
9. Zheng, G.; Patolsky, F.; Cui, Y.; Wang, W.U.; Lieber, C.M. Multiplexed electrical detection of cancer markers with nanowire sensor arrays. *Nat. Biotechnol.* **2005**, *23*, 1294–1301. [CrossRef]
10. Patolsky, F.; Zheng, G.; Hayden, O.; Lakadamyali, M.; Zhuang, X.; Lieber, C.M. Electrical detection of single viruses. *Proc. Natl. Acad. Sci. USA* **2004**, *101*, 14017–14022. [CrossRef]
11. Tintelott, M.; Pachauri, V.; Ingebrandt, S.; Vu, X.T. Process variability in top-down fabrication of silicon nanowire-based biosensor arrays. *Sensors* **2021**, *21*, 5153. [CrossRef]
12. Willems, K.; Van Meervelt, V.; Wloka, C.; Maglia, G. Single-molecule nanopore enzymology. *Phil. Trans. R. Soc. B* **2017**, *372*, 20160230. [CrossRef] [PubMed]

13. Kolmogorov, M.; Kennedy, E.; Dong, Z.; Timp, G.; Pevzner, P.A. Single-molecule protein identification by sub-nanopore sensors. *PLoS Comput. Biol.* **2017**, *13*, e1005356. [CrossRef] [PubMed]

14. Duan, N.D.; Li, C.; Song, M.; Wang, Z.; Zhu, C.; Wu, S. Signal amplification of SiO2 nanoparticle loaded horseradish peroxidase for colorimetric detection of lead ions in water. *Stereochim. Acta A Mol. Biomol. Spectrosc.* **2022**, *265*, 120342. [CrossRef] [PubMed]

15. Nayak, S.; Kale, P.; Balasubramanian, P. Inhibition assays of horseradish peroxidase by hexavalent chromium and other heavy metals. *Int. J. Environ. Anal. Chem.* **2020**. [CrossRef]

16. Rahemi, V.; Trashin, S.; Hafideddine, Z.; van Doorslaer, S.; Meynen, V.; Gorton, L.; de Wael, K. Amperometric Flow-Injection Analysis of Phenols Induced by Reactive Oxygen Species Generated under Daylight Irradiation of Titania Impregnated with Horseradish Peroxidase. *Anal. Chem.* **2020**, *92*, 3643–3649. [CrossRef]

17. Gezer, P.G.; Hsiao, A.; Kokini, J.L.; Liu, G.L. Simultaneous transfer of noble metals and three-dimensional micro- and nanopatterns onto zein for fabrication of nanophotonic platforms. *J. Mater. Sci.* **2016**, *51*, 3806–3816. [CrossRef]

18. Oo, S.Z.; Siitonen, S.; Kontturi, V.; Eustace, D.A.; Charlton, M.D.B. Disposable gold coated pyramidal SERS sensor on the plastic platform. *Opt. Express* **2016**, *24*, 724–731. [CrossRef]

19. Perdomo, J.; Hinkers, H.; Sundermeier, C.; Seifert, W.; Martínez Morell, O.; Knoll, M. Miniaturized real-time monitoring system for l-lactate and glucose using microfabricated multi-enzyme sensors. *Biosens. Bioelectron.* **2000**, *15*, 515–522. [CrossRef]

20. Perney, N.M.; Baumberg, J.J.; Zoorob, M.E.; Charlton, M.D.; Mahnkopf, S.; Netti, C.M. Tuning localized plasmons in nanostructured substrates for surface-enhanced Raman scattering. *Opt. Express* **2006**, *14*, 847–857. [CrossRef]

21. Balezin, M.; Baryshnikova, K.V.; Kapitanova, P.; Evlyukhin, A.B. Electromagnetic properties of the great pyramid: First multipole resonances and energy concentration. *J. Appl. Phys.* **2018**, *124*, 034903. [CrossRef]

22. Ivanov, Y.D.; Pleshakova, T.O.; Shumov, I.D.; Kozlov, A.F.; Ivanova, I.A.; Valueva, A.A.; Ershova, M.O.; Tatur, V.Y.; Stepanov, I.N.; Repnikov, V.V.; et al. AFM study of changes in properties of horseradish peroxidase after incubation of its solution near a pyramidal structure. *Sci. Rep.* **2021**, *11*, 9907. [CrossRef] [PubMed]

23. Kiselyova, O.I.; Yaminsky, I.V. Atomic Force Microscopy of Protein Complexes. In *Atomic Force Microscopy. Methods in Molecular Biology*; Braga, P.C., Ricci, D., Eds.; Humana Press: Totowa, NJ, USA, 2004; Volume 242, pp. 217–230.

24. Laskowski, D.; Strzelecki, J.; Pawlak, K.; Dahm, H.; Balter, A. Effect of ampicillin on adhesive properties of bacteria examined by atomic force microscopy. *Micron* **2018**, *112*, 84–90. [CrossRef] [PubMed]

25. Ivanov, Y.; Tatur, V.; Pleshakova, T.; Shumov, I.; Kozlov, A.; Valueva, A.; Ivanova, I.; Ershova, M.; Ivanova, N.; Repnikov, V.; et al. Effect of Spherical Elements of Biosensors and Bioreactors on the Physicochemical Properties of a Peroxidase Protein. *Polymers* **2021**, *13*, 1601. [CrossRef] [PubMed]

26. Ivanov, Y.D.; Pleshakova, T.O.; Shumov, I.D.; Kozlov, A.F.; Ivanova, I.A.; Valueva, A.A.; Tatur, V.Y.; Smelov, M.V.; Ivanova, N.D.; Ziborov, V.S. AFM imaging of protein aggregation in studying the impact of knotted electromagnetic field on a peroxidase. *Sci. Rep.* **2020**, *10*, 9022. [CrossRef]

27. Kiselyova, O.I.; Yaminsky, I.V.; Ivanov, Y.D.; Kanaeva, I.P.; Kuznetsov, V.Y.; Archakov, A.I. AFM study of membrane proteins, cytochrome P450 2B4, and NADPH–Cytochrome P450 reductase and their complex formation. *Arch. Biochem. Biophys.* **1999**, *371*, 1–7. [CrossRef]

28. Pleshakova, T.O.; Kaysheva, A.L.; Shumov, I.D.; Ziborov, V.S.; Bayzyanova, J.M.; Konev, V.A.; Uchaikin, V.F.; Archakov, A.I.; Ivanov, Y.D. Detection of hepatitis C virus core protein in serum using aptamer-functionalized AFM chips. *Micromachines* **2019**, *10*, 129. [CrossRef]

29. Ivanov, Y.D.; Danichev, V.V.; Pleshakova, T.O.; Shumov, I.D.; Ziborov, V.S.; Krokhin, N.V.; Zagumenniy, M.N.; Ustinov, V.S.; Smirnov, L.P.; Shironin, A.V.; et al. Irreversible chemical AFM-based fishing for detection of low-copied proteins. *Biochem. (Moscow) Suppl. Ser. B Biomed. Chem.* **2013**, *7*, 46–61. [CrossRef]

30. Sanders, S.A.; Bray, R.C.; Smith, A.T. pH-Dependent properties of a mutant horseradish peroxidase isoenzyme C in which Arg38 has been replaced with lysine. *Eur. J. Biochem.* **1994**, *224*, 1029–1037. [CrossRef]

31. Enzymatic Assay of Peroxidase (EC 1.11.1.7) 2,2′-Azino-Bis(3-Ethylbenzthiazoline-6-Sulfonic Acid) as a Substrate Sigma Prod. No. P-6782. Available online: https://www.sigmaaldrich.com/RU/en/technical-documents/protocol/protein-biology/enzyme-activity-assays/enzymatic-assay-of-peroxidase-abts-as-substrate (accessed on 18 February 2022).

32. Ivanov, Y.D.; Malsagova, K.A.; Bukharina, N.S.; Vesnin, S.G.; Usanov, S.A.; Tatur, V.Y.; Lukyanitsa, A.A.; Ivanova, N.D.; Konev, V.A.; Ziborov, V.S. Radiothermometric Study of the Effect of Amino Acid Mutation on the Characteristics of the Enzymatic System. *Diagnostics* **2022**, *12*, 943. [CrossRef]

33. Pershin, S.M. A New of the Action of EMF on Water/Aqueous Solutions, Taking into Account the Quantum Differences of the Ortho/Para of Spin Isomers of H2O. Online Biophysical Blog. Available online: http://www.biophys.ru/archive/sarov2013/proc-p17.pdf (accessed on 7 April 2022).

34. Minin, I.V.; Minin, O.V.; Yue, L. Electromagnetic properties of the pyramids from the photonics position. *Russ. Phys. J.* **2020**, *62*, 1763–1769. [CrossRef]

35. Suvak, V.A.; Tokmakova, O.A.; Gromov, V.A. Calculation and modeling of monostatic EPR of simple bodies. *Electron. Means Control. Syst.* **2015**, *1*, 36–39.

36. Calafiore, G.; Koshelev, A.; Darlington, T.P.; Borys, N.J.; Melli, M.; Polyakov, A.; Cantarella, G.; Allen, F.I.; Lum, P.; Wong, E.; et al. Campanile near-field probes fabricated by nanoimprint lithography on the facet of an optical fiber. *Sci. Rep.* **2017**, *7*, 1651. [CrossRef] [PubMed]